

Polychlorinated Trityl Radicals for Dynamic Nuclear Polarization: The Role of Chlorine Nuclei

Juan Carlos Paniagua,^b Verónica Mugnaini,^{c,d} Cristina Gabellieri,^a Miguel Feliz,^b Nans Roques,^c Jaume Veciana^{*c,d}, and Miquel Pons^{*a,b}

⁵ Received (in XXX, XXX) Xth XXXXXXXXX 200X, Accepted Xth XXXXXXXXX 200X

First published on the web Xth XXXXXXXXX 200X

DOI: 10.1039/b000000x

Polychlorinated trityl radicals bearing carboxylate substituents are water soluble persistent radicals that can be used for Dynamic Nuclear Polarization. In contrast to other trityl radicals, the polarization mechanism differs from the classical solid effect. DFT calculations performed to rationalize this behaviour support the hypothesis that polarization is transferred from the unpaired electron to chlorine nuclei and from these to carbon by spin diffusion. The marked differences observed between neutral and anionic forms of the radical will be discussed.

1. Introduction

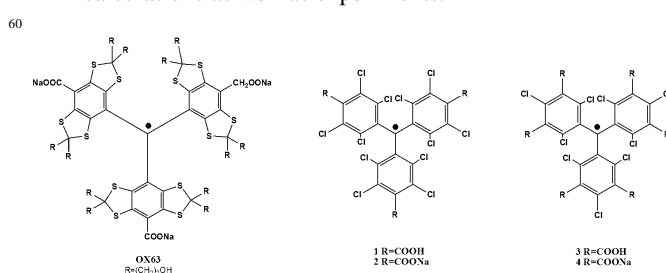
15 One of the main limitations of NMR is its low sensitivity associated with a very small population difference between different spin states at room temperature and achievable magnetic fields. The gyromagnetic ratio of the electron is 2640 times higher than that of carbon 13 nuclei resulting in a much larger polarization at the same temperature and magnetic field. The high electron polarization can be transferred to nuclei in the bulk of the sample by irradiating at the frequency of electronic spin resonances. This is the principle of Dynamic Nuclear Polarization (DNP).¹ The non-equilibrium nuclear polarization results in a much higher NMR sensitivity. In dissolution DNP experiments, enhanced nuclear polarization is generated at temperatures close to 1K in a solid sample containing a stable radical acting as polarizing agent and the molecule of interest in a glassing solvent. When the nuclear polarization has built up, the sample is quickly dissolved and shuttled to a conventional NMR instrument for observation.² Fast transfer is essential since magnetization is lost by relaxation.

The choice of the radical is crucial to determine the polarization transfer mechanism and the efficiency of the process.³ The main mechanisms for solid-state DNP are the thermal mixing/cross effects and the solid-effect. The former two mechanisms are operative when the width of the EPR line is larger than the nuclear frequency. The solid-effect is usually observed when the homogeneous EPR line-width of the radical is smaller than the nuclear Larmor frequency, as in the case of trityl radicals such as OX63 (Scheme 1), whose persistency is related to the bulky substituents sterically hindering the central sp² carbon where most of the spin density resides. When this mechanism is operating, optimal enhancement is achieved by irradiating at frequencies separated from the electron resonance frequency by the nuclear frequency.

We have recently described the use of water soluble polychlorotriphenylmethyl (PTM) radicals as polarizing agents in DNP experiments to enhance carbon-13 polarization.⁴ We have suggested that the electron

polarization could be initially transferred intramolecularly to chlorine nuclei and that the observed carbon polarization comes from the polarized chlorine nuclei *via* spin diffusion.

In this article we extend our results to include a comparison of radicals tri *para* carboxylic PTM (**1**) and its sodium salt (**2**); hexa *meta* carboxylic PTM (**3**) and its sodium salt (**4**) using DFT calculations as well as experiments.



Scheme 1. Structures of OX63 and the investigated polychlorinated radicals.

All PTM radical derivatives show high stability and persistency thanks to their unique structure. The six *ortho* chlorine atoms are located at ca. 3Å with respect to the central sp² carbon atom where most of the unpaired electron density is expected. The sterical hindrance ensures the persistence and the chemical stability of the radicals. The *para* or *meta* positions of the chlorinated phenyl rings can be occupied by distinct functional group(s), hence modulating the supramolecular interactions of these trigonal molecules. Namely, these radicals have been successfully used as robust open-shell organic synthons for the preparation of multidimensional networks showing magnetic ordering at low temperatures.⁵ The three phenyl rings assume a propeller-like conformation, with dihedral angles between the phenyl rings, as determined from the crystal structures, similarly to the ones reported for OX63.⁶ This high out-of-plane torsion of the phenyl rings causes in these radicals a decrease in the conjugation of the π -electron system and hence affects the spin density distribution.

2. Experimental and computational methods

Experimental methods. Substituted PTM radicals were synthesized as previously described.⁷ OX63 is a commercial (Oxford Molecular Biotoools) non-chlorinated trityl radical with carboxylate groups as sodium salts in the *para* position.

A Bruker Elexsys X-band instrument equipped with a rectangular standard cavity (TE 102) was used to record the EPR room temperature spectra.

Ex-situ DNP polarisation was performed using a HyperSense® DNP polariser (Oxford Instruments, UK).

Frequency calibration was done using the sodium salt of the radicals dissolved at 15 mM concentration in neat $1\text{-}^{13}\text{C}$ enriched pyruvic acid (Cortecnet). Pyruvic acid forms a glass and, in its enriched form, gives enough sensitivity to carry out frequency sweeps by detecting the carbon signal in solid state. For transfer experiments, $1\text{-}^{13}\text{C}$ pyruvate sodium salt, $2\text{-}^{13}\text{C}$ acetone, or ^{13}C urea (99% ^{13}C enriched, Sigma Aldrich) were dissolved in a 1 M mixture of $\text{H}_2\text{O}:\text{DMSO}$ (1:1) containing 15 mM of the radical of choice, polarised for 1.5 hour at 1.4 K while irradiating (100 mW power) at the microwave frequency corresponding at the first maximum of the microwave sweep of the corresponding radical. The polarised sample was then rapidly dissolved in 4ml methanol and transferred to a 5 mm tube placed inside the NMR spectrometer (500 MHz Varian Inova). A ^{13}C -NMR spectrum of the polarised solution was recorded employing a 90° RF pulse. This whole process took around 4 seconds. After decay of the polarisation, a thermal equilibrium spectrum was recorded for each sample (1024 transients) with a 20° flip angle. Data were analyzed by using VNMRJ Varian and MestreNova software. The enhancement factor was calculated by the ratio of the polarised signal to the thermal equilibrium multiplied by the square root of the number of scans.

Computational details. Relevant properties were calculated for the four radicals of Scheme 1 using Density Functional Theory (DFT). The hybrid exchange-correlation functional B3LYP⁸ was chosen, since it has proven to provide a rather accurate description of the electronic density at a much lower cost than high level quantum chemical methods.⁹ In every case all-electron calculations have been performed so as to get the correct nodal properties of the orbitals in the core region.

A crucial point for obtaining a reliable description of the core region with DFT methodology is to use a very fine quadrature grid for the numerical calculation of integrals over functionals. We had to use three computational packages to obtain the desired properties, due to limitations of each of them. Since their implemented grid systems were not completely equivalent, large grids of similar type were chosen. The reported Fermi contact couplings and spin dipole couplings were calculated with the Gaussian 09 rev. A.02 package¹⁰ using the ultrafine grid (a pruned grid with 99 radial shells around each atom, and 590 angular points in each shell).¹¹ The quadrupole coupling constant and g-tensors were obtained with the Orca 2.7 rev. 0 program¹² using grid 6 (Lebedev with 590 angular points) for the SCF iterations and grid 7 (Lebedev with 770 angular points) for the final point, and the Gauss-Chebyshev radial integration method.¹³ The

number of radial points is atom dependent, as specified in the user manual. In every case the tightest convergent option was chosen for the SCF convergence. The coupled-perturbed method has been used for evaluating the spin-orbit coupling.¹⁴ For obtaining starting symmetrized geometries and for some additional calculations the GAMESS ver. 12 Jan 2009 R3 package¹⁵ has also been used with 590 angular and 96 radial points.

Preliminary calculations with a 6-31G(d,p) basis set were used to obtain reasonable starting geometries.¹⁶ This basis set has been designed to provide a good description of properties dependent mostly on the valence region of the electron density. To calculate the hyperfine coupling constants, we used the IGLO basis set,¹⁷ specifically designed to reproduce such core properties and that covers all nuclei we are interested in. In order to check for convergence with the basis set level, calculations were performed with both the IGLO-II and IGLO-III sets. Both sets gave very similar results, indicating a good degree of convergence. Only the results with the larger set will be shown. In every case molecular geometries were optimized with the same basis set used for property calculations, so as to ensure that the electric field at the nuclei vanishes. Each radical has several conformations differing in the orientation of the rings and of the carboxyl groups. Some of them are symmetry equivalent and others have small energy differences. In these cases the most stable ones have been chosen. Their symmetry point group is C_3 for radical **1** and D_3 for the others.¹⁸

3. Results and discussion

3.1. X-band EPR in solution

Room temperature X-band EPR spectra have been recorded for the chlorinated compounds **1-4** in a mixture of $\text{H}_2\text{O}:\text{DMSO}$ 1:1 (Fig. 1).

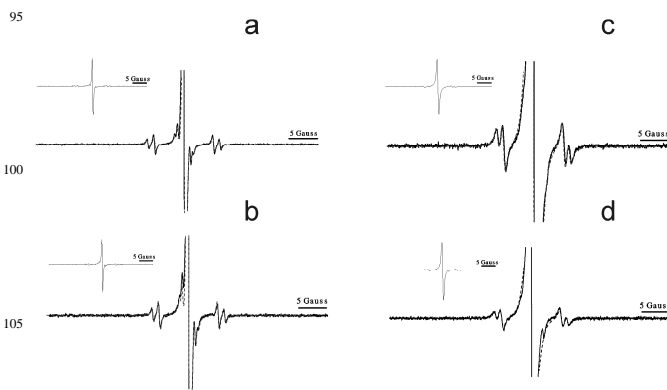


Figure 1. EPR X-band spectra in $\text{DMSO}:\text{H}_2\text{O}$ 1:1 at room temperature. a) **1**; b) **2**; c) **3**; d) **4**. Each simulated spectrum (dash gray line) is superimposed to the experimental one (solid black line) recorded at high MW power to see the ^{13}C hyperfine couplings. In the inset the full range experimental spectrum recorded under optimal power conditions.

Narrow EPR linewidths (less than 0.7G in the absence of oxygen) are observed for all the chlorinated compounds. The g-values for **1** and **2** (with three carboxylic substituents,

2.0029 and 2.0021 respectively) are lower than for **3** and **4** (with six carboxylic substituents, 2.0041 and 2.0034 respectively).¹⁹ As a reference the *g*-value of OX63 in H₂O:DMSO 1:1 is 2.0031 and the EPR linewidth is 0.2 G.

Thanks to the presence of large number of symmetry related carbons it is possible to measure the hyperfine couplings to carbon-13 nuclei at natural abundance, observed as satellite lines. The coupling to the central carbon could not be observed. This is probably due to fast relaxation because of the slow tumbling rate of the molecule in this viscous solvent under the used experimental conditions.²⁰ The largest observed coupling arise from the phenyl ¹³C bridgehead (*ipso*), followed by the phenyl ¹³C in *ortho* (2,6) with respect to the central carbon atom, followed by the coupling with the phenyl ¹³C in *para* (4) and *meta* (3,5) positions. Hyperfine couplings were accurately determined by simulation of the experimental spectra.²¹ Moreover, hyperfine couplings and *g*-values were computed for radicals **1-4** (see below). The experimental and calculated hyperfine couplings to carbon are compared in table 1.

Table 1. Experimental and calculated ¹³C-hyperfine coupling constants and *g*-values of PTM radicals **1-4** and OX63 in 1:1 DMSO:H₂O.

Position:	¹³ C Hyperfine couplings ^a /MHz				<i>g</i> -value ^b	
	1 (<i>ipso</i>)	2,6 (<i>ortho</i>)	3,5 (<i>meta</i>)	4 (<i>para</i>)		
1	exp. :	35.76	29.00	5.88	8.68	2.0029
	calc.:	-34.43	29.65	-6.14	7.74	
2	exp. :	35.62	29.12	5.88	8.68	2.0021
	calc.:	-34.09	29.18	-5.88	7.57	
3	exp. :	35.42	29.68	5.94	8.96	2.0041
	calc.:	-34.33	30.79	-5.94	9.12	
4	exp. :	35.48	29.4	5.6	8.12	2.0034
	calc.:	-35.55	30.27	-5.50	8.07	
OX63	exp. :	31.36	25.06	6.16	9.24	2.0031
	calc.:	-32.51	25.66	-5.07	5.90	

^a Hyperfine couplings are measured in absolute value. DFT calculations give also the sign. Experimental values were obtained by simulation of the experimental spectra including hyperfine couplings to the carbonyl carbons that were equal or smaller than those to *meta* carbons.

^b Experimental uncertainty is ±0.0003.

^c Ref.6

3.2. DNP experiments

As previously reported,⁴ carbon-13 DNP enhancements were observed using the sodium salts **2** and **4**. However, there are substantial differences between PTM and other trityl radicals, such as OX63.

The first one concerns the microwave frequencies at which optimal carbon-13 enhancements are observed. When the solid-effect mechanism is operative two maxima separated by 2*ν_C are expected. Indeed, for OX63 a frequency separation of 72 MHz was observed, consistent with twice the Larmor

frequency of carbon at 3.38T, using the radical dissolved in neat 1-¹³C-pyruvic acid at 1.5K. The separation of the two maxima for **2** and **4** in neat pyruvic acid was 124 and 136 MHz, respectively, and the two maxima are broader. These values indicate that carbons are not polarized by a direct solid-effect mechanism.

The second striking difference was observed in the case of **4**, where negative or positive DNP enhancements were observed, for distinct substrates or even for different ionization states of the same substrate.⁴ This effect was shown to be a genuine DNP effect as the sign was reversed by changing the irradiation frequency from the lower to the higher frequency side of the electronic resonance frequency.

A third peculiarity, not previously reported, is the very different enhancements obtained with the neutral or anionic forms of the radicals. Only a broad profile was observed when polarization of ¹³C-pyruvic acid was attempted using the protonated radicals **1** and **3** (results not shown). Attempts to polarize carbon nuclei using the protonated forms of the radicals and the frequencies optimized for their sodium salts resulted in weaker enhancements than with the sodium salts (Table 2).

Table 2. DNP enhancements after transfer^a

	1- ¹³ C Pyruvate	¹³ C Urea	2- ¹³ C Acetone
OX63^b	39214	12430	10863
1^c	198	2320	1509
2^b	29925	6392	4061
3^c	1780	1891	517
4^b	3026	2545	901

^a Enhancements were calculated as described in the experimental section

^b Ref.4

^c This work. Irradiation at the same frequency of the corresponding salt

In order to try to rationalize the origin of the singular DNP effects observed with PTM radicals, we have carried out detailed DFT calculations of the hyperfine couplings in four PTM radicals with distinct chlorine substituents and different ionization states.

3.3. DFT calculations

Figure 2 shows the optimized geometries and spin densities of radicals **1-4** computed using DFT and IGLO-III basis set.

Table 1 shows a comparison of calculated and experimental *g*-values and isotropic hyperfine couplings to carbons for PTM radicals. As a reference, the experimental values of OX63 measured by us in the same conditions are compared with the calculated values in reference 6.

DFT calculations accurately predict the different *g*-values of the the two families of PTM radicals. Hyperfine couplings are also well reproduced for all the aromatic carbons.

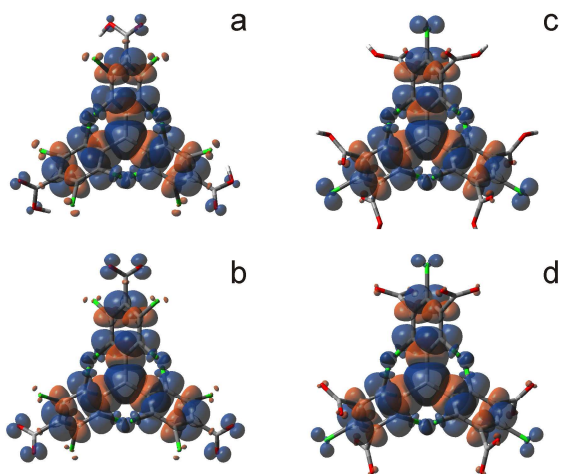


Figure 2. Optimized geometries and spin densities of PTM radicals. a) **1**; b) **2**; c) **3**; d) **4**. The largest spin density in chlorine atoms is in the *para* position of radical **3**, which also gives the largest hyperfine coupling. The isodensity surface has been drawn at 0.0005 a.u.

The good agreement between the calculated and experimental *g*-values and observed hyperfine couplings with carbon 13 provide a validation for the calculations. Hyperfine couplings with chlorine atoms are not observed in solution due to the fast relaxation of quadrupolar chlorine nuclei. However substantial couplings are predicted by the calculations. The calculated isotropic Fermi coupling and the principal components of the dipolar coupling tensor (including the isotropic and anisotropic terms) are given in Table 2. The anisotropic coupling is relevant since DNP is carried out in a solid glass sample.

Table 3 Calculated chlorine hyperfine couplings in PTM radicals **1-4**

		Fermi/MHz	D_{11} /MHz	D_{22} /MHz	D_{33} /MHz
1	Cl _{ortho}	0.35	-2.43	-0.41	3.19
	Cl _{meta}	0.15	-1.98	0.44	1.69
2	Cl _{ortho}	0.09	-2.11	-0.23	2.43
	Cl _{meta}	0.17	-1.62	0.30	1.50
3	Cl _{ortho}	0.24	-2.22	-0.37	2.83
	Cl _{para}	0.78	-2.96	-1.85	5.59
4	Cl _{ortho}	0.33	-1.95	-0.06	2.34
	Cl _{para}	0.3	-1.83	-0.92	3.05

The calculated isotropic hyperfine couplings to chlorine atoms are larger in the *ortho* and *para* positions than in *meta*, except for **2** where the Fermi coupling to the *ortho* chlorine is smaller. The calculated couplings to chlorine nuclei correlate well with the spin densities around these atoms shown in Figure 2. The unpaired spin densities near the *para* chlorine

atoms in radicals **3** and **4** are much higher than those in the *meta* chlorine atoms of **1** and **2**. Also the spin densities in the *para* chlorines is larger in **3** than in **4**. When the anisotropic coupling is considered, the distribution of values of the three principal components of the chlorine hyperfine coupling tensor in radicals **2** and **4** are very different. In the case of **2** for both the *ortho* and *meta* chlorine nuclei, the mean of D_{11} and D_{33} is close to D_{22} , i.e. the expected powder pattern of the hyperfine coupling to both chlorine atoms is rather symmetrical. In contrast, in the case of the *para* chlorine of **4**, the mean of D_{11} and D_{33} (+0.61 MHz) is substantially different from D_{22} (-0.92 MHz), indicating a very asymmetric powder pattern. Interestingly, only for radical **4** negative DNP enhancements have been observed.

When equivalent chlorine atoms of the free acids and the corresponding salts are compared, the three principal components are larger in magnitude in the free acids than in the sodium salts. However, the same trends concerning the symmetry of the powder distribution are observed for the free acids and the salts. In the hexacarboxylic radicals **3** and **4**, coupling to the *para* chlorine atoms is predicted to be larger than to those in *ortho*, in spite of a much larger distance to the sp^2 central carbon.

The calculations reveal that the large number of magnetically active, spin 3/2, chlorine nuclei located in the periphery of PTM radicals are effectively coupled to the unpaired electron and could be effectively polarized by irradiation at the proper microwave frequency. The chlorine nuclei could subsequently act as a source of polarization of other nuclei in the sample.

The reason for the marked difference between the protonated and anionic forms of the radicals is not obvious. Chlorine relaxation is expected to be slow in the solid sample. Short range magnetic ordering may result in a longer correlation time for electron exchange and may provide an additional relaxation mechanism for chlorine, which could quench DNP. Broadening of the NQR signal in *p*-Cl BDPA radical has been reported at temperatures below 3.2 K.²²

Intermolecular hydrogen bond formation is possible in the acids **1** and **3** but not in the salts. Previous observations from some of us showed that crystals of **3** show magnetic interactions (ferromagnetic or antiferromagnetic, depending on the solvate) arising from hydrogen bonded contacts between radicals.^{5,23}

The Larmor frequency at 3.38 T of ³⁵Cl is 14.1 MHz and that of ³⁷Cl is 11.7 MHz. Both isotopes have large quadrupolar moments of $-8.2 \times 10^{-30} \text{ m}^2$ and $-6.4 \times 10^{-30} \text{ m}^2$, respectively. Quadrupolar couplings of aromatic chlorinated molecules are typically around -70 MHz,²⁴ larger than the Zeeman chlorine frequency but neither interaction can be considered just as a perturbation of the other one. Under these conditions, multiple quantum transitions become allowed. Direct observation of forbidden transitions has been made in an oriented sodium chlorate single crystal and confirmed by exact calculations of the transition frequencies.²⁵ When dipolar couplings between spin 1/2 and quadrupolar nuclei are considered, one should

keep in mind that the quantization axes of chlorine and $\frac{1}{2}$ spins are not necessarily collinear.²⁶ The effect of quadrupolar nuclei in polycrystalline EPR spectra was calculated by Rollmann and Chan.²⁷ They noticed that transitions implying $|\Delta m| > 1$ were important in these systems.

For a cylindrically symmetric system in which the quadrupolar and Zeeman axes of chlorine were collinear, the transition frequencies would include simple additive combinations of the Zeeman multiple quantum terms and the quadrupolar frequencies. For other orientations the frequencies depend on the angle of the Zeeman and quadrupolar terms. Interestingly, the order of magnitude of the separation of the two microwave frequency maxima that give optimal DNP to carbons coincide with twice the frequency of the double quantum ^{35}Cl transition plus the expected isotropic quadrupolar energy splitting. With quadrupolar couplings in the range of -70 MHz to -80 MHz, the expected separations would be 126 MHz to 136 MHz, very close to the 124 MHz and 136 MHz observed in the case of **2** and **4** in neat pyruvic acid. The exact energy differences will depend on the orientation of the radical in the glass. A more detailed analysis, taking into account this orientational dependence is beyond the scope of this article but a broad maximum is expected.

Conclusions

Chlorinated trityl radicals are chemically stable and give narrow EPR lines in solution. DNP enhancement of carbon-13 nuclei has been demonstrated using polychlorinated derivatives **1-4**, differing in the position of chlorine atoms and of carboxylate/carboxylic groups. Maximum DNP enhancements are obtained with the sodium salts of the radicals. PTM derivative **2** shows a DNP efficiency comparable, although slightly lower, to the widely used OX63 radical. Derivative **4** has a lower efficiency but it shows striking supramolecular effects that may shed light on the details of the initial polarization transfer step with different substrates.

The microwave frequencies that give the maximum enhancement do not support the solid effect mechanism of other non-chlorinated trityl radicals. Instead, they suggest that carbon-13 polarization takes place by internuclear polarization from chlorine nuclei that are polarized by the electron through hyperfine coupling.

DFT calculations correctly reproduce the EPR g -values and hyperfine couplings to carbons that can be measured experimentally. Moreover they are able to supply the values of the hyperfine couplings to chlorines. These are large and dramatically sensitive to position as well as to the ionization state of the substituent. The *para* chlorine nuclei in **3** and **4** have the largest couplings, in spite of being the more distant to the centre of the radical, where most of the unpaired spin density is located. Hyperfine couplings predicted by the calculations show that there is an efficient way to hyperpolarize chlorine nuclei. The degree of polarization will also depend on the efficiency of the competing relaxation pathways. The relatively large paramagnetic density in the

peripheral chlorine nuclei may contribute to relaxation, specially if intermolecular interactions are favoured, e.g. by hydrogen bonding. This may contribute to the observed differences in the enhancements obtained with the tri *para* carboxylate (**2**) and hexa *meta* carboxylate PTMs (**4**) salts and also between these and their protonated forms (**1** and **3**).

Further experimental and theoretical work is in progress to try to advance towards the quantitative prediction of the observed effects.

One of the predictions of the indirect polarization model is that it should be short range, due to the low gyromagnetic ratio of chlorine, affecting only those nuclei that are close to the chlorine atoms in the glass. The fact that polarization takes place via chlorine nuclei implies that the irradiation frequency to enhance distinct nuclei would be the same. This may open the possibility of using chlorinated trityl groups as universal radicals for multinuclear applications or to enhance the sensitivity of low frequency nuclei.

Acknowledgments

We thank Dr. Maria Antonia Molins for support in the operation and maintenance of the Hypersense instrument, Malena Oliveros for the synthesis of the chlorinated radicals **1** and **2** and Dr. F. Mota for his help in solving computational problems. This work was partially supported by the MICINN-Spain, (BIO2007-63458, Project Consolider-C EMOCIONa, CTQ2006-06333/BQU, and LRB-ICTS), from the Generalitat de Catalunya, (2009SGR516 and 2009SGR1352) and from the Networking Research Center on Bioengineering, Biomaterials, and NanoMedicine (CIBER-BBN), promoted by ISCIII, Spain. V.M. acknowledges the MICINN-Spain for a Juan de la Cierva postdoctoral contract. Preliminary data were acquired in Birmingham with support from EU-NMR. Computational facilities provided by the Centre de Supercomputació de Catalunya (CESCA) through a grant from the Universitat de Barcelona are acknowledged.

Notes and references

^a Institute for Research in Biomedicine, Parc Científic de Barcelona, Baldiri Reixac, 10-12 08028-Barcelona, Spain . Fax: +34934039976; Tel: +34934034683; E-mail: mpons@ub.edu.

^b Universitat de Barcelona. Martí i Franquès 1-11 08028 Barcelona, Spain.

^c Institute of Materials Science of Barcelona (ICMAB-CSIC), Bellaterra, Spain. E-mail: vecianaj@icmab.es.

^d Networking Research Center on Bioengineering, Biomaterials, and NanoMedicine (CIBER-BBN), Bellaterra, Spain,

- 1 T. R. Carver, C. P. Slichter, *Phys. Rev.* 1953, **92**, 212; A. Abragam, M. Goldman, *Rep. Prog. Phys.* 1978, **41**, 395.
- 2 J. H. Ardenkjær-Larsen, F. Björn, A. Gram, G. Hansson, L. Hansson, M. H. Lerche, R. Servin, M. Thaning, K. Golman, *Proc. Natl. Acad. Sci. U.S.A.* 2003, **100**, 10158; A.-H. Emwas, M. Saunders, C. Ludwig, U. L. Günther, *Appl. Magn. Res.*, 2008, **34**, 483.
- 3 Th. Maly, G. T. Debelouchina, V. S. Bajaj, K.-N. Hu, C.-G. Joo, M. L. Mak-Jurkauskas, J. R. Sirigiri, P. C. A. van der Wel, J. Herzfeld, R. J. Temkin, R. G. Griffin *J. Chem. Phys.* 2008, **128**, 052211.

- 4 C. Gabellieri, V. Mugnaini, J. C. Paniagua, N. Roques, M. Oliveros, M. Feliz, J. Veciana, M. Pons, *Angew. Chem. Int. Ed.* In press.
- 5 D. Maspoch, N. Domingo, N. Roques, K. Wurst, J. Tejada, C. Rovira, D. Ruiz-Molina, J. Veciana, *Chem. Eur. J.* 2007, **13**, 8153; N. Roques, D. Maspoch, A. Dacu, K. Wurst, D. Ruiz-Molina, C. Rovira, J. Veciana, *Polyhedron* 2007, **26**, 1934; D. Maspoch, D. Ruiz-Molina, K. Wurst, N. Domingo, M. Cavallini, F. Biscarini, J. Tejada, C. Rovira, J. Veciana, *Nature Mat.*, 2003, 190.
- 6 M. K. Bowman, C. Mailer, H.J. Halpern, *J. Magn. Res.* 2005, **172**, 254.
- 7 D. Maspoch, N. Domingo, D. Ruiz-Molina, K. Wurst, G. Vaghan, J. Tejada, C. Rovira, J. Veciana, *Angew. Chem. Int. Ed.* 2004, **43**, 1828; N. Roques, D. Maspoch, K. Wurst, D. Ruiz-Molina, C. Rovira, J. Veciana, *Chem. Eur. J.* 2006, **12**, 9238.
- 8 A. D. Becke, *J. Chem. Phys.* 1993, **98**, 5648; C. Lee, W. Yang and R. G. Parr, *Phys. Rev. B* 1988, **37**, 785.
- 9 P. Schwerdtfeger, M. Pernpointner and J. K. Laerdahl, *J. Chem. Phys.* 1999, **111**, 3357; A. Rizzo, K. Ruud, T. Helgaker, P. Salek, H. Ågren, O. Vahtras, *Chem. Phys. Lett.* 2003, **372**, 377.
- 10 Gaussian 09, revision A.02, M. J. Frisch, G. W. Trucks, H. B. Schlegel, G. E. Scuseria, M. A. Robb, J. R. Cheeseman, G. Scalmani, V. Barone, B. Mennucci, G. A. Petersson, H. Nakatsuji, M. Caricato, X. Li, H. P. Hratchian, A. F. Izmaylov, J. Bloino, G. Zheng, J. L. Sonnenberg, M. Hada, M. Ehara, K. Toyota, R. Fukuda, J. Hasegawa, M. Ishida, T. Nakajima, Y. Honda, O. Kitao, H. Nakai, T. Vreven, J. A. Montgomery, Jr., J. E. Peralta, F. Ogliaro, M. Bearpark, J. J. Heyd, E. Brothers, K. N. Kudin, V. N. Staroverov, R. Kobayashi, J. Normand, K. Raghavachari, A. Rendell, J. C. Burant, S. S. Iyengar, J. Tomasi, M. Cossi, N. Rega, J. M. Millam, M. Klene, J. E. Knox, J. B. Cross, V. Bakken, C. Adamo, J. Jaramillo, R. Gomperts, R. E. Stratmann, O. Yazyev, A. J. Austin, R. Cammi, C. Pomelli, J. W. Ochterski, R. L. Martin, K. Morokuma, V. G. Zakrzewski, G. A. Voth, P. Salvador, J. J. Dannenberg, S. Dapprich, A. D. Daniels, O. Farkas, J. B. Foresman, J. V. Ortiz, J. Cioslowski, and D. J. Fox, Gaussian, Inc., Wallingford CT, 2009.
- 11 V. I. Lebedev and L. Skorokhodov, *Russian Acad. Sci. Dokl. Math.* 1992, **45**, 587.
- 12 ORCA version 2.7 rev. 0, F. Neese, Lehrstuhl fuer Theoretische Chemie, Institut fuer Physikalische und Theoretische Chemie, Universitaet Bonn, Germany, June 2009.
- 13 O. Treutler, R. Ahlrichs, *J. Chem. Phys.* 1994, **102**, 346; M. Krack, A. M. Köster, *J. Chem. Phys.* 1998, **108**, 3226.
- 14 F. Neese, *J. Chem. Phys.* 2007, **127**, 164112.
- 15 M. W. Schmidt, K. K. Baldrige, J. A. Boatz, S. T. Elbert, M. S. Gordon, J. J. Jensen, S. Koseki, N. Matsunaga, K. A. Nguyen, S. Su, T. L. Windus, M. Dupuis, J. A. Montgomery, *J. Comput. Chem.* 1993, **14**, 1347; M. S. Gordon, M. W. Schmidt, in *Theory and Applications of Computational Chemistry, the first forty years*, C. E. Dykstra, G. Frenking, K. S. Kim, G. E. Scuseria (editors), Elsevier, 2005, p 1167.
- 16 W. J. Hehre, R. Ditchfield and J. A. Pople, *J. Chem. Phys.* 1972, **56**, 2257; P. C. Hariharan and J. A. Pople, *Theoret. Chimica Acta* 1973, **28**, 213; M. M. Francl, W. J. Pietro, W. J. Hehre, J. S. Binkley, M. S. Gordon, D. J. DeFrees and J. A. Pople, *J. Chem. Phys.* 1982, **77**, 3654.
- 17 W. Kutzelnigg, U. Fleischer, M. Schindler, *The IGLO-Method: Ab Initio Calculation and Interpretation of NMR Chemical Shifts and Magnetic Susceptibilities*, Springer-Verlag, 1990, vol. 23.
- 18 The lower symmetry of **1** with respect to **2** is due to the presence of the proton in the carboxylic acid. Slightly different values are obtained by the two *ortho* and *meta* carbons of **1**. The reported values in table 1 are average values.
- 19 The uncertainty of *g*-values measured from CW X-band spectra is ± 0.0003 .
- 20 For other PTM derivatives, the coupling with the central carbon atom has been found to be around 30G (O. Armet, J. Veciana, C. Rovira, J. Riera, J. Castañer, E. Molins, J. Rius, C. Miravittles, S. Olivella, J. Brichtfeus, *J. Phys. Chem.* 1987, **91**, 5608). The reported coupling for OX63 is 23.96G.
- 21 Simulations made using SimFonia (Bruker).
- 22 T. Yoshioka, J. Yamauchi, H. Ohya-Nishiguchi, Y. Deguchi, *Bull. Chem.Soc. Japan*, 1975, **48**, 335.
- 23 N. Roques, D. Maspoch, N. Domingo, D. Ruiz-Molina, K. Wurst, J. Tejada, C. Rovira, J. Veciana *Chem. Commun.*, 2005, 4801.
- 24 E.A.C. Lucken, *Nuclear Quadrupole Coupling Constants*. Academic Press. London 1969; p 187
- 25 A.D. Bain, *Mol Phys.*, 2003, **101**, 3163; M.Khasawneh, J.S. Hartman, A.D. Bain, *Mol.Phys.*, 2004, **102**, 975.
- 26 D.L. VanderHart, H.S. Gutowsky, T.C. Farrar, *J. Am. Chem. Soc.* 1967, **89**, 5056; J.G. Hexem, M.H. Frey, S.J. Opella, *J. Chem. Phys.* 1982, **77**, 3847..
- 27 L.D. Rollmann, S.I. Chan, *J. Chem. Phys.* 1969, **50**, 3416.